

On the control of recurrent neural networks using constant inputs

Cyprien Tamekue, Ruiqi Chen and ShiNung Ching, *Senior Member, IEEE*

Abstract—This paper investigates the controllability properties of a general class of recurrent neural networks that are widely used for hypothesis generation in theoretical neuroscience, including the modeling of large-scale human brain dynamics. Our study focuses on the control synthesis of such networks using constant and piecewise constant inputs, motivated by emerging applications in non-invasive neurostimulation such as transcranial direct current stimulation (tDCS). The neural network model considered is a continuous Hopfield-type system with nonlinear activation functions and arbitrary input matrices representing interactions among multiple brain regions. Our main contribution is the formulation and solution of a control synthesis problem for these nonlinear systems. We provide a proper generalization of the variation of the constants formula that constitutes a novel representation of the system's state trajectory. This representation admits a verifiable condition on the existence of the constant control input to solve a short-time two-point boundary value problem in the state space. This formulation admits a synthesis for the input in question, which can be realized using modern algorithmic optimization tools. In the case of linear activation functions, this analysis and synthesis reduces to the verification of algebraic conditions on the system matrices. Simulation results are presented to illustrate the theoretical findings and demonstrate the efficacy of the proposed control strategies. These results offer a novel control synthesis for an important class of neural network models that may, in turn, enable the design of brain stimulation protocols to modulate whole-brain activity in therapeutic and cognitive enhancement applications.

Index Terms—Controllability, Control Synthesis, Nonlinear Control, Recurrent Neural Networks, Neurostimulation, Transcranial Direct Current Stimulation.

I. INTRODUCTION

NON-INVASIVE neurostimulation techniques, such as transcranial magnetic stimulation (TMS) and transcranial electrical stimulation (tES), are increasingly being used to modulate brain activity in order to achieve desired cognitive outcomes [2], [11], [15]. Conceptualizing the brain as a controlled dynamical system [22] offers a powerful framework for identifying key brain regions and networks [18] involved in specific cognitive functions and understanding how they can be modulated using targeted stimulation.

In this regard, there is strong potential at the intersection of network control theory and clinical and basic neuroscience.

This work is partially supported by grant R21MH132240 from the US National Institutes of Health to SC.

Cyprien Tamekue and ShiNung Ching are with the Department of Electrical and Systems Engineering, Washington University in St. Louis, St. Louis, 63130, MO, USA; Ruiqi Chen is with the Neurosciences Program in the Division of Biology and Biomedical Sciences, Washington University in St. Louis, St. Louis, 63130, MO, USA (e-mail: cyprien@wustl.edu, chen.ruiqi@wustl.edu, shinung@wustl.edu).

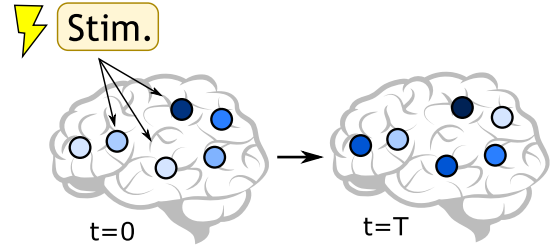


Fig. 1. We consider the control of Hopfield-type network models of the general form (1). We are motivated by emerging applications in neurostimulation involving the manipulation of brain networks by means of exogenous input.

For instance, there have been successes in the application of linear network control theory to optimize TMS, administered with a constant input over short time intervals [17]. Such applications target the control of specific brain regions based on structural network connectivity derived from diffusion spectrum imaging (DTI). Similarly, at an analysis level, linear network control theory has been employed in human neuroimaging studies, again by leveraging DTI-parameterized models [12]. In this latter study, the authors postulated how specific brain regions may be suitable targets for control based on advantageous controllability properties relative to their potential actuation. While these earlier studies [12], [17] have provided valuable insights by using linear network control theory and structural connectivity data to understand brain dynamics, they are limited in key respects. Foremost, by virtue of linearity, they are only assured to provide local characterizations. In [17], it is shown that these local analyses can offer some predictive power over functional changes in nonlinear models. However, the changes considered are in terms of low-dimensional correlation metrics between brain areas (network nodes), as opposed to specific configurations in state space. In contrast, our goal is to enable formal control analysis and synthesis to induce arbitrary network states in the presence of full nonlinearity, which is likely essential for understanding how different brain dynamics mediate cognitive function.

Indeed, the need for more biologically realistic, nonlinear models of large-scale brain dynamics has been appreciated [3] as a precursor for the application of control theory to cognitive neuroscience. Among the paradigms in this regard are whole-brain Mesoscale Individualized NeuroDynamic (MINDy) models [5], [20]. Our previous works have demonstrated the validity and utility of MINDy models as a generative tool for understanding the relationship between individual-

ized neural architectures and neural dynamics in both resting-state [20], [21] and cognitive task contexts [19]. The MINDy models derived from single-subject resting-state brain imaging data operate at a macroscale level, where each node represents a distinct brain region. A given model captures the temporal evolution of brain activity and the non-linear interactions between hundreds of brain regions, taking the form of a nonlinear dynamical system of continuous-time Hopfield-type recurrent neural networks [13]. All (intrinsic) parameters—the decay and connectivity matrices and the transfer function parameters—are directly estimated from brain activity time series so that the resulting models predict future brain activity, providing a more accurate and biologically plausible representation of large-scale brain dynamics.

A MINDy model belongs to the more general class of Hopfield-type recurrent neural networks, which will constitute the focus of our study herein. Specifically, we consider a model of interconnected neural masses associated with d regions, described by a set of nonlinear differential equations that represent the dynamics of each region's state over time. The dynamic for the i -th region in this network evolves as

$$\begin{aligned} \dot{x}_i(t) &= -\alpha_i x_i(t) + \sum_{j=1}^d W_{ij} f_j(x_j(t)) + \sum_{j=1}^k b_{ij} u_j \\ x_i(0) &= x_i^0 \end{aligned} \quad (1)$$

where $k \in \mathbb{N}^*$ satisfies $k \leq d$, $x_i(t)$ denotes the i -th region's state at time $t \geq 0$, $\alpha_i > 0$ is a positive parameter reflecting the rate at which the current state of the i -th region decays, u_j are constant control inputs, b_{ij} represent coupling coefficients between control inputs and neurons, W_{ij} is a real constant that weights the connection from the j -th region to the i -th region, and f_j is the activation function of the j -th region.

The study of neural networks, such as (1), has long been a topic of great interest for researchers seeking to understand complex dynamical behaviors and their associated control mechanisms, [1], [10], [13], [24], [27], [28]. Among the various properties investigated, controllability—the ability to steer a network from one state to another within a finite time—stands out for its significant theoretical and practical implications. As highlighted earlier, in fields such as neuroengineering and brain stimulation, particularly transcranial electrical stimulation (tES) with direct current (stimulation via a constant input), the operative issue is to determine a constant input that can drive the state of the network (1) to a desired target state—within the state space—over a short time horizon (Figure 1). Such capability would presents a promising avenue for developing stimulation protocols tailored to achieve specific therapeutic outcomes [9], such as altering the excitability of motor cortex [2].

In previous works such as [10], [24], [27], [28], controllability or stability properties of equations as (1) have been considered in the full-actuated configuration when $d = k$ and $B := (b_{ij}) = \text{Id}$ or in the specific cases of B belonging to an open dense subset of $\mathcal{M}_{d,k}(\mathbb{R})$. In the current study, the input matrix $B := \in \mathcal{M}_{d,k}(\mathbb{R})$ is general, and assumptions on the activation functions are relaxed to that well-used in the literature in studying neural networks. The general assumption

on B and the complexity arising from the inherent nonlinear dynamics present significant challenges, and systematic solutions for the *control synthesis* problem are not readily available in the current literature. To address this challenge, we derive a novel expression for the hidden state $x(t)$, the solution to (2) that provides analytical leverage in determining feasibility of control with respect to constant inputs. Furthermore, under this representation, we synthesize a constant input that steers the system from an initial to a desired target state within the state space over a short period of time. From this derivation, we then provide a piecewise constant input for large periods of time. In the case of linear activation functions, this reduces to a simpler algebraic synthesis for an arbitrary positive time horizon under some conditions on the matrices of decay coefficients and synaptic weight. Numerical examples with simulation results are presented to illustrate the effectiveness of the obtained results.

The remainder of the paper is organized as follows. In the next section, we introduce the general notations that will be used throughout the paper. In Section II, we present our settings, reformulating equation (1) in a form more suitable for controllability analysis and providing the main results related to the solution representation. Section III addresses the control synthesis problem and is divided into two parts: Section III-A focuses on the case of linear activation functions, while Section III-B extends the analysis to general nonlinear activation functions. Section IV provides numerical examples and simulation results to illustrate the effectiveness of the proposed approaches. Finally, in Section V, we summarize the main results and outline potential directions for future research. Technical proofs of some results are deferred to the Appendix.

Notation 1. In this paper, \mathbb{Z} stands to the set of integers, \mathbb{N}^* denote the set of positive integers and $\mathbb{N} = \mathbb{N}^* \cup \{0\}$. For all $a, b \in \mathbb{N}$, we denote by $\llbracket a, b \rrbracket = \mathbb{N} \cap [a, b]$. For all $d, k \in \mathbb{N}^*$, we denote by $\mathcal{M}_{d,k}(\mathbb{R})$ the set of $d \times k$ matrices with real coefficients. \mathbb{R}^d denotes the d -dimensional real column vector and $\mathcal{L}(\mathbb{R}^d)$ the space of linear maps on \mathbb{R}^d that we identify, in the usual way, with $\mathcal{M}_d(\mathbb{R})$ the set of squared matrices of order d with real coefficients. For all $(x, y) \in \mathbb{R}^d \times \mathbb{R}^d$, we denote by $\|x\|_2$ the Euclidean norm of x and by $\langle x, y \rangle$ the scalar product of x and y . We denote the identity matrix in $\mathcal{M}_d(\mathbb{R})$ by Id , and for every matrix $A \in \mathcal{M}_d(\mathbb{R})$, $\|A\| = \sup\{\|Ax\|_2 \mid x \in \mathbb{R}^d, \|x\|_2 = 1\}$ denotes the spectral norm of A . For a symmetric matrix $M \in \mathcal{M}_d(\mathbb{R})$, $\lambda_{\min}(M)$ and $\lambda_{\max}(M)$ denote respectively its smaller and largest eigenvalues. For ease of notation, a diagonal matrix $\Gamma = \text{diag}(\gamma_1, \gamma_2, \dots, \gamma_d) \in \mathcal{M}_d(\mathbb{R})$, will simply denoted as $\Gamma = (\gamma_i \delta_{i,j})$, where $\delta_{i,j}$ is the usual Kronecker symbol.

II. REPRESENTATION OF SOLUTIONS

For our purpose of studying the controllability of (1), it is convenient to write it in an abstract form as follows.

$$\dot{x}(t) = N(x(t)) + Bu, \quad x(0) = x^0 \quad (2)$$

where $x = (x_1, x_2, \dots, x_d)^\top \in \mathbb{R}^d$ is the state's vector, $x^0 = (x_1^0, \dots, x_d^0)^\top \in \mathbb{R}^d$ is the initial state, $u = (u_1, \dots, u_k)^\top \in$

\mathbb{R}^k is a constant control, $B = (b_{ij}) \in \mathcal{M}_{d,k}$ is the input matrix, $D = (\alpha_i \delta_{i,j}) \in \mathcal{M}_d(\mathbb{R})$ is the decay matrix, $W = (W_{ij}) \in \mathcal{M}_d(\mathbb{R})$ is the connectivity matrix and $f : \mathbb{R}^d \rightarrow \mathbb{R}^d$ given by $f(x) = (f_1(x_1), f_2(x_2), \dots, f_d(x_d))^T$ is the firing rate function of the network. The drift term N is given by

$$N(x) = -Dx + Wf(x) \quad \forall x \in \mathbb{R}^d. \quad (3)$$

Assumptions II.1. Throughout the following, unless otherwise stated, we assume that for every $i \in \llbracket 1, d \rrbracket$, the activation function $f_i : \mathbb{R} \rightarrow \mathbb{R}$ is a C^2 non-decreasing, globally 1-Lypchitz function on \mathbb{R} with a bounded second derivative, and satisfies $f_i(0) = 0$. The latter is without loss of generality since we may always take for every $s \in \mathbb{R}$, $\tilde{f}_i(s) = f_i(s) - f_i(0)$ and set $\tilde{B}u = Bu - Wf(0)$ as the new input to equation (2). Finally, for the sake of simplicity in the presentation, one also assumes that $\|f'_i\|_\infty = 1$. Indeed, as long as $\|f'_i\|_\infty \neq 0$, we can always define an activation function $\tilde{f}_i(s) = f_i(\lambda s)$ with $\lambda = 1/\|f'_i\|_\infty$ and $s \in \mathbb{R}$.

Notation 2. Throughout the following, we set $A := -D + W$, where D is the decay matrix and W is the connectivity matrix, both appearing in (3).

Recall that the nonlinear vector field N is globally Lipschitz on \mathbb{R}^d (see, for instance, Lemma A.1). Denoting by $\Phi_t : \mathbb{R}^d \rightarrow \mathbb{R}^d$ its flow at $t \in \mathbb{R}$, it follows that the family $\{\Phi_t \mid t \in \mathbb{R}\}$ is a one parametric subgroup of $\text{Diff}(\mathbb{R}^d)$, the group of all diffeomorphism of \mathbb{R}^d . Note that for any $x^0 \in \mathbb{R}^d$, $\Phi_t(x^0)$ is the unique solution to (2) when the control $u = 0$, namely

$$\frac{\partial \Phi_t(x^0)}{\partial t} = N(\Phi_t(x^0)), \quad \Phi_0(x^0) = x^0. \quad (4)$$

Let denote by Ψ_t be the inverse of Φ_t for every $t \in \mathbb{R}$. Then, for every $x^0 \in \mathbb{R}^d$, it holds $\Psi_t(x^0) = \Phi_{-t}(x^0)$ and

$$\frac{\partial \Psi_t(x^0)}{\partial t} = -N(\Psi_t(x^0)), \quad \Psi_0(x^0) = x^0. \quad (5)$$

In particular, for a fixed $t \in \mathbb{R}$, Φ_t and Ψ_t are differentiable at every $x \in \mathbb{R}^d$ and $y = \Phi_t(x)$, respectively. Moreover, it follows from Lemma A.2 that if we use $D\Phi_t(x)$ and $D\Psi_t(y)$ to denote respectively the evaluation of these differentials at any $x \in \mathbb{R}^d$ and $y = \Phi_t(x)$, then $D\Phi_t(x)$ is a well-defined invertible matrix for any $x \in \mathbb{R}^d$ and every $t \in \mathbb{R}$, and it holds

$$[D\Phi_t(x)]^{-1} = D\Psi_t(y). \quad (6)$$

The classical theory of ordinary differential equations (ODE) can be invoked to justify the existence and uniqueness of solutions to (2). In this work, we represent the system's state trajectory in a form reminiscent of that of linear time-invariant systems and has been first evoked in [26, Theorem 4.4.] to the author's knowledge. Indeed, the representation we propose here is particularly noteworthy because, in the specific case of linear activation functions, it naturally aligns with the variation of the constants formula—without requiring any nontrivial manipulations. From this perspective, the proposed representation and approach is a proper generalization of variation of constants formula to the case of models of the form (2).

The first main result of this paper is about solution representation, and it states as follows

Theorem II.2. *Let $T > 0$. For any $x_0 \in \mathbb{R}^d$ and every $u \in \mathbb{R}^k$, the solution $x \in C^3([0, T]; \mathbb{R}^d)$ of (2) can be expressed as*

$$x(t) = \Phi_t \left(x^0 + \int_0^t D\Psi_s(x(s)) Buds \right) \quad (7)$$

for every $0 \leq t \leq T$.

Proof. Let $y : t \in [0, T] \mapsto y(t) \in \mathbb{R}^d$ be such that $x(t) = \Phi_t(y(t))$ is the solution of (2). Then, y is at least derivable w.r.t. t and it holds

$$N(x(t)) + Bu = \dot{x}(t) = N(x(t)) + D\Phi_t(y(t))\dot{y}(t). \quad (8)$$

Using (6), one finds that y solves the following.

$$\dot{y}(t) = D\Psi_t(x(t))Bu, \quad y(0) = x^0. \quad (9)$$

Integrating (9) over $[0, t]$ yields (7). Conversely, if (7) holds, then $x \in C^2([0, T]; \mathbb{R}^d)$ by composition and $x(0) = \Phi_0(x^0) = x^0$. Letting

$$z(t) := x^0 + \int_0^t D\Psi_s(x(s)) Buds \quad (10)$$

and deriving (7) w.r.t. t yields to

$$\begin{aligned} \dot{x}(t) &= \partial_t \Phi_t(z(t)) + D\Phi_t(z(t))D\Psi_t(x(t))Bu \\ &= N(\Phi_t(z(t))) + Bu = N(x(t)) + Bu \end{aligned} \quad (11)$$

by $x(t) = \Phi_t(z(t))$ and $D\Phi_t(z(t))D\Psi_t(x(t)) = \text{Id}$. Since (11) defines a continuous function in t , one deduces that x given by (7) belongs to $C^3([0, T]; \mathbb{R}^d)$ and solves (2). \square

In the case where the dynamics are linear, this representation reduces to the familiar form as follows:

Corollary II.3. *Let $T > 0$. Assume that the activation function f_i is linear for every $i \in \llbracket 1, d \rrbracket$. Then, for every $x^0 \in \mathbb{R}^d$ and $u \in \mathbb{R}^k$, the solution $x \in C^\infty([0, T]; \mathbb{R}^d)$ of (2) can be expressed as*

$$x(t) = e^{tA}x^0 + \int_0^t e^{(t-s)A} Buds \quad \forall t \in [0, T]. \quad (12)$$

Proof. In this case, $N(x) = Ax$ where A is introduced in Notation 2. One has $\Phi_t = e^{tA}$ and $D\Psi_s(x(s)) = e^{-sA}$. One gets immediately from (7) that

$$\begin{aligned} x(t) &= e^{tA} \left(x^0 + \int_0^t e^{-sA} Buds \right) \\ &= e^{tA}x^0 + \int_0^t e^{(t-s)A} Buds \end{aligned} \quad (13)$$

completing the proof of the corollary. \square

To end this section, let us present a second representation of the solution to (2), which will be useful in our later derivations of necessary and sufficient conditions for control existence. The proof is similar to that of Theorem II.2.

Theorem II.4. *Let $T > 0$. For any $x_0 \in \mathbb{R}^d$ and every $u \in \mathbb{R}^k$, the solution $x \in C^3([0, T]; \mathbb{R}^d)$ of (2) can be expressed as*

$$x(t) = \Psi_{T-t} \left(\Phi_T(x^0) + \int_0^t D\Phi_{T-s}(x(s)) Buds \right) \quad (14)$$

for every $0 \leq t \leq T$.

As in Corollary II.3, one can easily check that if the activation function f_i is linear, then (14) naturally coincides with (12). Indeed, $N(x) = Ax$ where A is introduced in Notation 2. One has $\Phi_T = e^{TA}$, $\Psi_{T-t} = e^{-(T-t)A}$ and $D\Phi_{T-s}(x(s)) = e^{(T-s)A}$. The result is then immediate.

III. CONTROLLABILITY OF THE NEURAL NETWORKS WITH STEP CONTROL

We discuss in this section the controllability properties of (2) with step control. As recalled in the introduction, the ability to manipulate neural networks (2) with step control is of great interest in the application, e.g., of non-invasive neurostimulation techniques such as tDCS (stimulation with a constant input) to modulate brain activity.

We recall that a step function on $[0, T]$ is a piecewise constant function defined on $[0, T]$. Therefore, of particular interest are constant functions on $[0, T]$.

Let us introduce the following.

Definition 3 (Step controllability). Let $T > 0$. System (2) is step controllable over the time interval $[0, T]$ if, for all $x^0, x^1 \in \mathbb{R}^d$, there exists a step function u on $[0, T]$ such that the solution of (2) with $x(0) = x^0$ satisfies $x(T) = x^1$.

A. The case of linear activation functions

To understand how the controllability of the nonlinear system (2) can be addressed with constant control, it is useful to first examine the corresponding linear model. In this case, the linear neural network is controllable in \mathbb{R}^d over the time interval $[0, T]$ (for any $T > 0$) if and only if the well-known Kalman rank condition for controllability is satisfied. The invertibility of the controllability Gramian further guarantees the controllability of the linear system in \mathbb{R}^d over the interval $[0, T]$. Moreover, the latter approach allows for synthesizing a *time-varying* control $\bar{u} \in L^\infty((0, T); \mathbb{R}^k)$ with minimal $L^2((0, T); \mathbb{R}^k)$ energy, which steers any $x^0 \in \mathbb{R}^d$ to any $x^1 \in \mathbb{R}^d$ within time T , see, for instance, [7].

However, this synthesis does not systematically extend to *constant control* capable of achieving the same objective. If the system is controllable, and we assume the existence of a constant input $\tilde{u} \in \mathbb{R}^k$ that steers the system from $x^0 \in \mathbb{R}^d$ to $x^1 \in \mathbb{R}^d$ over the interval $[0, T]$, then it must satisfy

$$(e^{TA} - \text{Id}) B \tilde{u} = A (x^1 - e^{TA} x^0). \quad (15)$$

However, (15) does not systematically admit a solution $\tilde{u} \in \mathbb{R}^k$, as shown by the following result.

Lemma III.1. Let $d, k \in \mathbb{N}^*$ with $k \leq d$. There exist matrices $A \in \mathbb{R}^{d \times d}$ and $B \in \mathbb{R}^{d \times k}$, such that the linear system $\dot{x}(t) = Ax(t) + Bu(t)$, $x(0) = x^0 \in \mathbb{R}^d$, is controllable, but there exists $x^1 \in \mathbb{R}^d$ that cannot be reachable with any nonzero constant control $\tilde{u} \in \mathbb{R}^k$.

Proof. Assume $d = k$ and $B = \text{Id}$. The system is controllable for any matrix $A \in \mathbb{R}^{d \times d}$ with some $u \in L^1((0, T); \mathbb{R}^k)$, by the Kalman condition. Let $x^0, x^1 \in \mathbb{R}^d$. If there exists a constant control $\tilde{u} \in \mathbb{R}^k$ such that the solution of the

linear system $\dot{x}(t) = Ax(t) + Bu(t)$ with $x(0) = x^0$ satisfies $x(T) = x^1$, then \tilde{u} solves (15). Define $z^1 := x^1 - e^{TA}x^0 \neq 0$ (otherwise, $\tilde{u} = 0$ solves (15)). Now, assume there exists $\ell \in \mathbb{Z}, \ell \neq 0$, such that $i2\pi\ell/T$ is an eigenvalue of A , and A is diagonalizable. Assume z^1 lies in the eigenspace corresponding to the eigenvalue $i2\pi\ell/T$, i.e., $Az^1 = (i2\pi\ell/T)z^1 \neq 0$. Expanding \tilde{u} in the basis of eigenvectors of A gives

$$\tilde{u} = c_1 v + \sum_{k=2}^d c_k v_k, \quad c_k \in \mathbb{R}$$

where v is the eigenvector for $i2\pi\ell/T$, and v_k are the eigenvectors for other eigenvalues $\lambda_k \in \mathbb{C}$. Then,

$$(e^{TA} - \text{Id})\tilde{u} = \sum_{k=2}^d c_k (e^{T\lambda_k} - 1)v_k = (i2\pi\ell/T)z^1. \quad (16)$$

Since $\langle z^1, v_k \rangle = 0$ for all $k \in \llbracket 2, d \rrbracket$, (16) implies $\|z^1\|_2 = 0$, which is a contradiction. \square

Therefore, Lemma III.1 suggests that the controllability of a linear system does not necessarily imply the existence of a *constant control* that solves the control objective.

Our primary goal in this section is to synthesize constant control to (2) when f_i is linear without assuming that the system is controllable. Thus, in the remainder of this section (and only here), we assume that the activation function f_i is linear for all $i \in \llbracket 1, d \rrbracket$, so that for every $x \in \mathbb{R}^d$, the vector field is given by $N(x) = Ax$, where $A = -D + W$.

Theorem III.2. Let $T > 0$ and $x^0, x^1 \in \mathbb{R}^d$. Assume either that $\|W\| < \lambda_{\min}(D)$, or that for any $\ell \in \mathbb{Z}$, $\lambda = i\frac{2\pi\ell}{T}$ is not an eigenvalue of the matrix A . Then, $x(T) = x^1$ if and only if $u \in \mathbb{R}^k$ satisfies

$$Bu = (e^{TA} - \text{Id})^{-1} A (x^1 - e^{TA}x^0) =: I. \quad (17)$$

Moreover, if (17) has at least a solution, $u = B^+I$ is the least-norm constant control among those controls. Here B^+ is the Moore-Penrose pseudo-inverse of the matrix B .

Remark III.3. For a full actuated linear control system, i.e., $k = d$ and $B = \text{Id}$ or a full row rank matrix $B \in \mathcal{M}_{d,k}(\mathbb{R})$, then (17) has at least one solution $u \in \mathbb{R}^k$.

Proof of Theorem III.2. By Corollary II.3, the solution $x \in C^\infty([0, T]; \mathbb{R}^d)$ of (2) with a constant control $u \in \mathbb{R}^k$ is given by

$$x(t) = e^{tA} + \int_0^t e^{(t-s)A} ds Bu. \quad (18)$$

If $\|W\| < \lambda_{\min}(D)$, then from inequality (80) of Lemma A.4, one deduces that the matrix $e^{TA} - \text{Id}$ is invertible and $(e^{TA} - \text{Id})^{-1}$ commutes with A by the Neumann expansion lemma. Whereas if $\|W\| \geq \lambda_{\min}(D)$ and $\lambda = i\frac{2\pi\ell}{T}$ is not an eigenvalue of A for any $\ell \in \mathbb{Z}$, then 1 is not an eigenvalue of e^{TA} . It follows that the matrix $e^{TA} - \text{Id}$ is invertible, but $(e^{TA} - \text{Id})^{-1}$ does not necessarily commute with A . In both cases, I as in (17) is well-defined in \mathbb{R}^d .

Let us now show that $x(T) = x^1$ is equivalent to (17). Firstly, if $x(T) = x^1$, then one obtains immediately (17) from (18). Conversely, if (17) is satisfied, then one gets

$$\begin{aligned} x(T) &= e^{TA}x^0 + \int_0^T Ae^{sA}ds (e^{TA} - \text{Id})^{-1} (x^1 - e^{TA}x^0) \\ &= e^{TA}x^0 + (e^{TA} - \text{Id}) (e^{TA} - \text{Id})^{-1} (x^1 - e^{TA}x^0) \\ &= x^1 \end{aligned} \quad (19)$$

whenever $\|W\| < \lambda_{\min}(D)$. While for $\|W\| \geq \lambda_{\min}(D)$, one lets $t = T$ in (18), and replace Bu by (17) to obtain

$$A(x(T) - x^1) = 0 \quad (20)$$

and then $x(T) = x^1$ since 0 is not an eigenvalue of A .

The last part of the theorem follows immediately since if $Bu = I$ has at least one solution $u \in \mathbb{R}^k$, then $\bar{u} = B^+I \in \mathbb{R}^k$ is the solution with the least-norm. \square

Remark III.4. In Theorem III.2, the assumption $\lambda = i2\pi\ell/T$ is not an eigenvalue of A for every $\ell \in \mathbb{Z}$ when $\|W\| \geq \lambda_{\min}(D)$ prohibits the matrix A to be skew-symmetric. Furthermore, in the case of $\|W\| = \lambda_{\min}(D)$, the matrix A cannot be skew-symmetric unless all the coefficients of the decay matrix D are equal. Otherwise, from $A^T = -A$, one gets $W + W^T = 2D$, and

$$2\lambda_{\max}(D) = \|W + W^T\| \leq 2\|W\| = 2\lambda_{\min}(D)$$

which is inconsistent. Finally, in the case of $\|W\| \geq \lambda_{\min}(D)$, if W is symmetric, then the matrix $e^{TA} - \text{Id}$ is invertible whenever 0 is not an eigenvalue of A .

Remark III.5 (On the condition on eigenvalues of A). Notice that to get (17), one solves equation $x(T) = x^1$ where $x(\cdot)$ is given by (12) assuming that $u \in \mathbb{R}^k$ is constant. Set $z^1 := x^1 - e^{TA}x^0 \neq 0$ (otherwise, $u = 0$ solves the control objective) so that this equation yields to

$$(e^{TA} - \text{Id})Bu = Az^1. \quad (21)$$

If there exists $\ell \in \mathbb{Z}$ such that $i2\pi\ell/T$ is an eigenvalue of A , then (17) does not make sense whenever $\|W\| \geq \lambda_{\min}(D)$. Nevertheless, (21) has at least one solution $u \in \mathbb{R}^k$ if

$$Az^1 \in \text{Im}[(e^{TA} - \text{Id})B]. \quad (22)$$

In this case, a constant control input that solves the control objective is taken as the one with the minimal Euclidean norm. It is given by

$$u = [(e^{TA} - \text{Id})B]^+ Az^1 \quad (23)$$

where M^+ is the Moore–Penrose pseudo-inverse of the matrix M . Furthermore, if $Az^1 \notin \text{Im}[(e^{TA} - \text{Id})B]$, then (21) has no solution. Lemma III.1 shows that this situation may happen.

B. The case of nonlinear activation functions

Theorem III.2 suggests that the controllability properties of (2) with constant control is related to the properties of the differential of the drift term N (Ax in the linear case) and the properties of the flow Φ_t and the inverse flow Ψ_t in general.

1) *Control synthesis Part I:* The following is the main result of this section, and it holds under Assumption II.1. It is based on the solution representation of (2) provided in Theorem II.2.

Theorem III.6. Let $T > 0$ and $x^0, x^1 \in \mathbb{R}^d$. Assume either that $\|W\| < \lambda_{\min}(D)$, or that for any $\ell \in \mathbb{Z}$, $\lambda = i\frac{2\pi\ell}{T}$ is not an eigenvalue of the matrix $DN(x^1)$. If $x(T) = x^1$ is achieved, then a corresponding control $u \in \mathbb{R}^k$ if it exists, must satisfy

$$(\text{Id} - \mathcal{D}_T(x^1)\zeta(T))Bu = \mathcal{D}_T(x^1)(\Psi_T(x^1) - x^0). \quad (24)$$

Here letting $\mathcal{B}_T(x^1) := DN(\Psi_T(x^1))$, one has

$$\mathcal{D}_T(x^1) := D\Phi_T(\Psi_T(x^1)) \left(e^{T\mathcal{B}_T(x^1)} - \text{Id} \right)^{-1} \mathcal{B}_T(x^1) \quad (25)$$

and the matrix $\zeta(T)$ is defined in Proposition III.7 below.

Before proving Theorem III.6, let us prove the following key results.

Proposition III.7. Let $T > 0$. For all $x_0 \in \mathbb{R}^d$ and $u \in \mathbb{R}^k$, the solution $x \in C^3([0, T]; \mathbb{R}^d)$ of (2) can be expanded as

$$x(t) = \Phi_t \left(x^0 + \sum_{n=0}^{\infty} \frac{t^{n+1} Z_t^n}{(n+1)!} P_t B u - \zeta(t) B u \right) \quad (26)$$

for all $t \in [0, T]$. Here $P_t := D\Psi_t(x(t))$, $\zeta(t) := \xi(t) + \chi(t)$ and

$$\xi(t) = \sum_{n=1}^{\infty} \int_0^t \frac{s^{n+1}}{(n+1)!} \left[\frac{d}{ds} Z_s^n \right] P_s ds \quad (27)$$

$$\chi(t) = \sum_{n=1}^{\infty} \int_0^t \frac{s^n}{n!} Z_s^{n-1} D^2 \Psi_s(x(s)) \dot{x}(s) ds \quad (28)$$

where $Z_t := DN(\Psi_t(x(t)))$ and $D^2 \Psi_s(x(s))$ is the hessian matrix of Ψ_s at $x(s)$.

Proof. Letting $P_s = D\Psi_s(x(s))$. Via a double integration by parts, one gets from Theorem II.2 that

$$\begin{aligned} x(t) &= \Phi_t \left(x^0 + \int_0^t s' P_s B u ds \right) \\ &= \Phi_t \left(- \int_0^t \frac{s^2}{2} \left[\frac{d}{ds} Z_s \right] P_s B u ds \right. \\ &\quad - \int_0^t s D^2 \Psi_s(x(s)) \dot{x}(s) B u ds \\ &\quad - \int_0^t \frac{s^2}{2} Z_s D^2 \Psi_s(x(s)) \dot{x}(s) B u ds + x^0 \\ &\quad \left. + t P_t B u + \frac{t^2}{2} Z_t P_t B u + \int_0^t \frac{s^2}{2} Z_s^2 P_s B u ds \right) \end{aligned} \quad (29)$$

from which one performs another integration by parts on the last integral in (29) and so on to obtain (26), (27) and (28). The series (26), (27), and (28) are well-defined by Lemma A.5. \square

Remark III.8. The matrices $\xi(t)$ and $\chi(t)$ contain the Hessian matrix $D^2 f$ of the vector field f as a multiplicative factor under the integral sign. In particular, if f_i is linear, then $\zeta(t) = 0 = \chi(t)$ and (26) coincides with (12).

Lemma III.9. For all $x, y \in \mathbb{R}^d$ and $t \in \mathbb{R}$, it holds

$$DN(y)D\Phi_t(\Psi_t(y)) = D\Phi_t(\Psi_t(y))DN(\Psi_t(y)). \quad (30)$$

$$DN(x)D\Psi_t(\Phi_t(x)) = D\Psi_t(\Phi_t(x))DN(\Phi_t(x)). \quad (31)$$

Proof. Since $\Phi_t : \mathbb{R} \rightarrow \mathbb{R}$ and $\Psi_t : \mathbb{R} \rightarrow \mathbb{R}$ are differentiable for every $t \in \mathbb{R}$ and satisfies (4) and (5) respectively, one finds for every $x, y \in \mathbb{R}^d$

$$\partial_t D\Phi_t(\Psi_t(y)) = DN(v)D\Phi_t(\Psi_t(y)). \quad (32)$$

$$\partial_t D\Psi_t(\Phi_t(x)) = -DN(x)D\Psi_t(\Phi_t(x)). \quad (33)$$

On the other hand, from $\Phi_t(\Psi_t(y)) = y$, one gets successively that $D\Phi_t(\Psi_t(y))D\Psi_t(y) = \text{Id}$ and

$$\partial_t D\Phi_t(\Psi_t(y)) = D\Phi_t(\Psi_t(y))DN(\Psi_t(y)). \quad (34)$$

using (33). While from $\Psi_t(\Phi_t(x)) = x$, one gets successively that $D\Psi_t(\Phi_t(x))D\Phi_t(x) = \text{Id}$ and

$$\partial_t D\Psi_t(\Phi_t(x)) = -D\Psi_t(\Phi_t(x))DN(\Phi_t(x)). \quad (35)$$

using (32). Finally, (32) and (34) yield to (30) while (33) and (35) yield to (31). \square

Lemma III.10. Let $x^1 \in \mathbb{R}^d$ and $T > 0$. Then, the matrix $e^{TDN(\Psi_T(x^1))} - \text{Id}$ is invertible if and only if the matrix $e^{TDN(x^1)} - \text{Id}$ is invertible.

Proof. Letting $\mathcal{B}_T(x^1) := DN(\Psi_T(x^1))$ and $Y_T(x^1) := (e^{T\mathcal{B}_T(x^1)} - \text{Id})D\Psi_T(x^1)$, one finds

$$\begin{aligned} Y_T(x^1) &= \sum_{n=1}^{\infty} \frac{T^n DN(\Psi_T(x^1))^n}{n!} D\Psi_T(x^1) \\ &= D\Psi_T(x^1) \sum_{n=1}^{\infty} \frac{T^n DN(x^1)^n}{n!} \\ &= D\Psi_T(x^1)(e^{TDN(x^1)} - \text{Id}) \end{aligned} \quad (36)$$

where in the second equality we used identity (31) applied with $t = T$ and $x = \Psi_T(x^1)$. It follows that

$$(e^{T\mathcal{B}_T(x^1)} - \text{Id}) = D\Psi_T(x^1)(e^{TDN(x^1)} - \text{Id})D\Phi_T(\Psi_T(x^1)).$$

This completes the proof since $D\Psi_T(x^1)$ and $D\Phi_T(\Psi_T(x^1))$ are invertible. \square

Let us now present the proof of Theorem III.6.

Proof of Theorem III.6. Set $\mathcal{B}_T(x^1) := DN(\Psi_T(x^1))$. From Lemma A.6, one has that if $\|W\| < \lambda_{\min}(D)$ then $e^{TDN(x^1)} - \text{Id}$ is invertible by the Neumann expansion lemma. Whereas in the case of $\|W\| \geq \lambda_{\min}(D)$, the assumption on the eigenvalues of $DN(x^1)$ ensures that $e^{TDN(x^1)} - \text{Id}$ is invertible. In both cases, $e^{T\mathcal{B}_T(x^1)} - \text{Id}$ is invertible by Lemma III.10, and the matrix $\mathcal{D}_T(x^1)$ introduced in (25) is well-defined.

Letting $t = T$ in (26), one gets from $x(T) = x^1$ that

$$\begin{aligned} DN(\Psi_T(x^1))(\Psi_T(x^1) - x^0) &= -DN(\Psi_T(x^1))\zeta(T)Bu \\ &+ \sum_{n=0}^{\infty} \frac{T^{n+1}}{(n+1)!} DN(\Psi_T(x^1))^{n+1} D\Psi_T(x^1)Bu \\ &= -DN(\Psi_T(x^1))\zeta(T)Bu \\ &+ (e^{T\mathcal{B}_T(x^1)} - \text{Id})D\Psi_T(x^1)Bu \end{aligned} \quad (37)$$

where $\mathcal{B}_T(x^1) := DN(\Psi_T(x^1))$. Since $[D\Psi_T(x^1)]^{-1} = D\Phi_T(\Psi_T(x^1))$, (37) yields

$$\begin{aligned} D\Phi_T(\Psi_T(x^1)) \left(e^{T\mathcal{B}_T(x^1)} - \text{Id} \right)^{-1} \mathcal{B}_T(x^1) (\Psi_T(x^1) - x^0) &= \\ Bu - D\Phi_T(\Psi_T(x^1)) \left(e^{T\mathcal{B}_T(x^1)} - \text{Id} \right)^{-1} \mathcal{B}_T(x^1) \zeta(T) Bu. \end{aligned} \quad (38)$$

It follows from (38) that $u \in \mathbb{R}^k$ is a solution of

$$[\text{Id} - \mathcal{D}_T(x^1)\zeta(T)]Bu = \mathcal{D}_T(x^1)(\Psi_T(x^1) - x^0) \quad (39)$$

where $\mathcal{D}_T(x^1)$ is defined as in (25). This completes the proof of the theorem. \square

Remark III.11. If f_i is linear, then the control synthesis in Theorem III.6 naturally coincides with that provided in Theorem III.2. Indeed, in this case, one has $\xi(T) = 0 = \chi(T)$ so that $\zeta(T) = 0$. One also has $\mathcal{B}_T(x^1) = A$, $\Psi_T(x^1) = e^{-TA}x^1$, $D\Phi_T(\Psi_T(x^1)) = e^{TA}$ so that (24) is identical to (17).

Proposition III.12. There exists $\bar{T} > 0$ such that for every $T \in (0, \bar{T}]$, under hypotheses of Theorem III.6, if $x(T) = x^1$ is achieved, then a corresponding control $u \in \mathbb{R}^k$ satisfies

$$Bu = [\text{Id} - \mathcal{D}_T(x^1)\zeta(T)]^{-1} \mathcal{D}_T(x^1)(\Psi_T(x^1) - x^0). \quad (40)$$

Here $\mathcal{D}_T(x^1)$ is defined as in (25).

Proof. It follows from Lemma A.5 that $\zeta(t) := \xi(t) + \chi(t)$ satisfies

$$\zeta(t) \underset{t \sim 0}{=} O(t^3). \quad (41)$$

One deduces that there exists $\bar{T} > 0$ such that for every $T \in (0, \bar{T}]$, it holds

$$\| \mathcal{D}_T(x^1)\zeta(T) \| < 1. \quad (42)$$

Therefore, the matrix $\text{Id} - \mathcal{D}_T(x^1)\zeta(T)$ is invertible, and the result follows from Theorem III.6. \square

Remark III.13. It is important to emphasize that in Proposition III.12, the condition that $T > 0$ is sufficiently small is a sufficient but not a necessary condition for ensuring the invertibility of the matrix $\text{Id} - \mathcal{D}_T(x^1)\zeta(T)$. For instance, when the activation function f_i is linear, the matrix remains invertible for any $T > 0$ since, in this case, $\zeta(T) = 0$.

The following result is immediate and provides a control synthesis with a step control for a large time horizon.

Corollary III.14. Let $\tau > \bar{T}$ where $\bar{T} > 0$ is chosen as in Proposition III.12. If there exists $u \in \mathbb{R}^k$ solution of (40) with $T \in (0, \bar{T}]$, then $u^* : [0, \tau] \rightarrow \mathbb{R}^k$ defined by

$$u^*(s) = \begin{cases} 0 & \text{if } 0 \leq s < \tau - T \\ u & \text{if } \tau - T \leq s \leq \tau \end{cases} \quad (43)$$

is a step control that steers the solution of (2) from $x^0 \in \mathbb{R}^d$ to $x^1 \in \mathbb{R}^d$ over the time interval $[0, \tau]$.

Let us illustrate the practical effectiveness of Proposition III.12 with several remarks.

Remark III.15. Observe that the control synthesis in Proposition III.12 is feedback-based, as $\zeta(T)$ incorporates the state $x(s)$ within the integral. However, for a sufficiently small time

horizon $T > 0$, if it exists, the feedforward control input $\tilde{u} \in \mathbb{R}^k$, solving

$$B\tilde{u} = \mathcal{D}_T(x^1)(\Psi_T(x^1) - x^0) =: I \quad (44)$$

provides a first approximation to the control input $u \in \mathbb{R}^k$ that solves (40). By (25), one has

$$I = D\Phi_T(\Psi_T(x^1)) \left(e^{T\mathcal{B}_T(x^1)} - \text{Id} \right)^{-1} \mathcal{B}_T(x^1)(\Psi_T(x^1) - x^0). \quad (45)$$

where $\mathcal{B}_T(x^1) = DN(\Psi_T(x^1))$. It follows that if $I \in \text{Im}(B)$, then (44) has at least one solution, and the constant control $\tilde{u} = B^+I \in \mathbb{R}^k$ is the least-norm solution to (44), and serves as a first approximation to the constant control $u \in \mathbb{R}^k$ synthesized in Proposition III.12. This control \tilde{u} approximately steers the solution of (2) from x^0 to x^1 over the time interval $[0, T]$, provided $T > 0$ is sufficiently small. For more details on the accuracy of this approximation, we refer the reader to Section IV, where numerical simulations are presented.

Interestingly, the control $\tilde{u} \in \mathbb{R}^k$ is actually a solution of

$$\left(e^{T\mathcal{B}_T(x^1)} - \text{Id} \right) D\Psi_T(x^1)B\tilde{u} = \mathcal{B}_T(x^1)(\Psi_T(x^1) - x^0). \quad (46)$$

Hence, similar to the analysis performed in Remark III.5, one can study the eigenvalues of $DN(x^1)$ —by Lemma III.10—to derive more general conditions that guarantee the existence of $\tilde{u} \in \mathbb{R}^k$ satisfying (46) when $\|W\| \geq \lambda_{\min}(D)$.

Remark III.16. For a full actuated nonlinear control system, i.e., $k = d$ and $B = \text{Id}$ or a full row rank matrix $B \in \mathcal{M}_{d,k}(\mathbb{R})$, then (44) has at least one solution $\tilde{u} \in \mathbb{R}^k$.

Remark III.17. For a large time horizon $T > 0$, a feedforward control that approximately solves the control objective can be synthesized as a step function as follows. One let $\tau > 0$ small enough and one considers $u_* : [0, T] \rightarrow \mathbb{R}^k$ defined by

$$u_*(s) = \begin{cases} 0 & \text{if } 0 \leq s < T - \tau \\ \tilde{u} & \text{if } T - \tau \leq s \leq T \end{cases} \quad (47)$$

where $\tilde{u} \in \mathbb{R}^k$ is defined as in Remark III.15.

2) *Control synthesis Part 2:* In contrast to the linear case presented in Theorem III.2, where one has a necessary and sufficient condition for the derivation of the control synthesis that solves the control objective, Theorem III.6 provides a different perspective. It offers a necessary condition on a constant control $u \in \mathbb{R}^k$ that steers the solution of (2) from an initial state $x^0 \in \mathbb{R}^d$ to a final state $x^1 \in \mathbb{R}^d$ over the time interval $[0, T]$.

In this section, based on the second representation of the solution of (2) given in Theorem II.4, one seeks to provide a necessary and sufficient condition on the control synthesis as in the linear case.

The following is the main result of this section, and it holds under Assumption II.1. It is based on the solution representation of Theorem II.4.

Theorem III.18. *Let $T > 0$ and $x^0, x^1 \in \mathbb{R}^d$. Assume either that $\|W\| < \lambda_{\min}(D)$, or that for any $\ell \in \mathbb{Z}$, $\lambda = i\frac{2\pi\ell}{T}$ is not*

an eigenvalue of the matrix $DN(x^0)$. Then, $x(T) = x^1$ if and only if $u \in \mathbb{R}^k$ satisfies

$$\left[\text{Id} - \mathcal{C}_T(x^0)\varphi(T) \right] Bu = \mathcal{C}_T(x^0)(x^1 - \Phi_T(x^0)) \quad (48)$$

where the matrix $\varphi(T)$ is defined in Proposition III.19 below. Letting $\mathcal{A}_T(x^0) := DN(\Phi_T(x^0))$, one has

$$\mathcal{C}_T(x^0) := D\Psi_T(\Phi_T(x^0)) \left(\text{Id} - e^{-T\mathcal{A}_T(x^0)} \right)^{-1} \mathcal{A}_T(x^0). \quad (49)$$

Before proving Theorem III.18, let us provide the following key results where the proof is identical to that of Proposition III.7.

Proposition III.19. *Let $T > 0$. For any $x_0 \in \mathbb{R}^d$ and every $u \in \mathbb{R}^k$, the solution $x \in C^3([0, T]; \mathbb{R}^d)$ of (2) can be expanded at time $t = T$ as*

$$x(T) = \sum_{n=0}^{\infty} (-1)^n \frac{T^{n+1} DN(\Phi_T(x^0))^n}{(n+1)!} D\Phi_T(x^0)Bu + \Phi_T(x^0) - \varphi(T)Bu. \quad (50)$$

Here $Q_{T-s} := D\Phi_{T-s}(x(s))$, $\varphi(T) := \kappa(T) + \eta(T)$ and

$$\kappa(T) = \sum_{n=1}^{\infty} (-1)^n \int_0^T \frac{(T-s)^{n+1}}{(n+1)!} \left[\frac{d}{ds} Z_{T-s}^n \right] Q_{T-s} ds. \quad (51)$$

$$\eta(T) = \sum_{n=1}^{\infty} (-1)^{n-1} \int_0^T \frac{(T-s)^n}{n!} Z_{T-s}^{n-1} D^2\Phi_{T-s}(x(s)) \dot{x}(s) ds \quad (52)$$

where $Z_{T-s} := DN(\Phi_{T-s}(x(s)))$ and $D^2\Phi_{T-s}(x(s))$ is the hessian matrix of Φ_{T-s} at $x(s)$.

Remark III.20. As in Lemma A.5, one can prove that

$$\kappa(T) \underset{T \sim 0}{=} O(T^3) \underset{T \sim 0}{=} \eta(T) \quad (53)$$

for every $T > 0$.

One also has the following key result.

Lemma III.21. *Let $x^0 \in \mathbb{R}^d$ and $T > 0$. Then the matrix $\text{Id} - e^{-T DN(\Phi_T(x^0))}$ is invertible if and only if the matrix $\text{Id} - e^{-T DN(x^0)}$ is invertible.*

Proof. Letting $\mathcal{A}_T(x^0) := DN(\Phi_T(x^0))$ and $Y_T(x^0) := (\text{Id} - e^{-T\mathcal{A}_T(x^0)})D\Phi_T(x^0)$, one finds

$$\begin{aligned} Y_T(x^0) &= \sum_{n=1}^{\infty} \frac{(-T)^n DN(\Phi_T(x^0))^n}{n!} D\Phi_T(x^0) \\ &= D\Phi_T(x^0) \sum_{n=1}^{\infty} \frac{(-T)^n DN(x^0)^n}{n!} \\ &= D\Phi_T(x^0)(\text{Id} - e^{-T DN(x^0)}) \end{aligned} \quad (54)$$

where in the second equality we used identity (30) applied with $t = T$ and $y = \Phi_T(x^0)$. It follows that

$$(\text{Id} - e^{-T\mathcal{A}_T(x^0)}) = D\Phi_T(x^0)(\text{Id} - e^{-T DN(x^0)})D\Psi_T(\Phi_T(x^0)).$$

This completes the proof since the matrices $D\Phi_T(x^0)$ and $D\Psi_T(\Phi_T(x^0))$ are invertible. \square

Proof of Theorem III.18. First of all, let $\mathcal{A}(x^0) := DN(x^0)$. From inequality (94) of Lemma A.6 one has that if

$\|W\| < \lambda_{\min}(D)$ then $e^{T\mathcal{A}(x^0)} - \text{Id}$ is invertible so that $\text{Id} - e^{-T\mathcal{A}(x^0)} = e^{-T\mathcal{A}(x^0)} \left(e^{T\mathcal{A}(x^0)} - \text{Id} \right)$ is invertible and its inverse commutes with $\mathcal{A}(x^0)$ by the Neumann expansion lemma. Whereas in the case of $\|W\| \geq \lambda_{\min}(D)$, the assumption on the eigenvalues of $\mathcal{A}(x^0)$ ensures that $\text{Id} - e^{-T\mathcal{A}(x^0)}$ is invertible while its inverse does not necessary commutes with $\mathcal{A}(x^0)$. In both cases, the matrix $\mathcal{C}_T(x^0)$ introduced in (49) is well-defined by Lemma III.10.

Let us show that $x(T) = x^1$ is equivalent to (48). On the one hand, it follows from (50) that if $x(T) = x^1$ then

$$\begin{aligned} DN(\Phi_T(x^0))(x^1 - \Phi_T(x^0)) &= -DN(\Phi_T(x^0))\zeta(T)Bu \\ &- \sum_{n=0}^{\infty} \frac{(-T)^{n+1}}{(n+1)!} DN(\Phi_T(x^0))^{n+1} D\Phi_T(x^0)Bu \\ &= -DN(\Phi_T(x^0))\zeta(T)Bu \\ &+ \left(\text{Id} - e^{-T\mathcal{A}_T(x^0)} \right) D\Phi_T(x^0)Bu \end{aligned} \quad (55)$$

where $\mathcal{A}_T(x^0) := DN(\Phi_T(x^0))$. Since $[D\Phi_T(x^0)]^{-1} = D\Psi_T(\Phi_T(x^0))$, (55) yields to

$$\left[\text{Id} - \mathcal{C}_T(x^0)\zeta(T) \right] Bu = \mathcal{C}_T(x^0)(x^1 - \Phi_T(x^0)) \quad (56)$$

where $\mathcal{C}_T(x^0)$ is defined as in (49). This completes the proof of sufficiency. Assume now that $u \in \mathbb{R}^k$ is a solution of (48). It follows that

$$\mathcal{C}_T(x^0)\zeta(T)Bu = Bu - \mathcal{C}_T(x^0)(x^1 - \Phi_T(x^0)). \quad (57)$$

From (50), one deduces that

$$\mathcal{C}_T(x^0)\zeta(T)Bu = Bu - \mathcal{C}_T(x^0)(x(T) - \Phi_T(x^0)). \quad (58)$$

Identifying (57) with (58), one gets

$$\mathcal{A}_T(x^0)(x(T) - x^1) = 0. \quad (59)$$

Since the matrix $\text{Id} - e^{-T\mathcal{A}_T(x^0)}$ is invertible, 0 is not an eigenvalue of $\mathcal{A}_T(x^0)$ so that $\mathcal{A}_T(x^0)$ is also invertible. It follows from (59) that $x(T) = x^1$. This completes the proof of the necessary part and, therefore, of the theorem. \square

Remark III.22. If f_i is linear, then the control synthesis in Theorem III.18 naturally coincides with that provided in Theorem III.2. Indeed, in this case, one has $\kappa(T) = 0 = \eta(T)$ so that $\varphi(T) = 0$. One also has $\mathcal{A}_T(x^0) = A$, $\Phi_T(x^0) = e^{TA}x^0$, $D\Psi_T(\Phi_T(x^0)) = e^{-TA}$ so that (48) is identical to (17).

For a small time horizon, one has the following result.

Proposition III.23. *There exists $\bar{T} > 0$ such that for every $T \in (0, \bar{T}]$, under hypotheses of Theorem III.18, $x(T) = x^1$ if and only if $u \in \mathbb{R}^k$ is the solution of*

$$Bu = \left[\text{Id} - \mathcal{C}_T(x^0)\varphi(T) \right]^{-1} \mathcal{C}_T(x^0)(x^1 - \Phi_T(x^0)). \quad (60)$$

Proof. It follows from Remark III.20 that $\varphi(T) = \kappa(T) + \eta(T)$ satisfies

$$\varphi(T) \underset{T \rightarrow 0}{=} O(T^3). \quad (61)$$

One deduces that there exists $\bar{T} > 0$ such that for every $T \in (0, \bar{T}]$, it holds

$$\| \mathcal{C}_T(x^0)\varphi(T) \| < 1. \quad (62)$$

Therefore, the matrix $\text{Id} - \mathcal{C}_T(x^0)\varphi(T)$ is invertible, and the result follows by Theorem III.18. \square

The following result provides a control synthesis with a step control for a large time horizon.

Corollary III.24. *Let $\tau > \bar{T}$ where $\bar{T} > 0$ is chosen as in Proposition III.23. If there exists $u \in \mathbb{R}^k$ solution of (60) with $T \in (0, \bar{T}]$, then $u^* : [0, \tau] \rightarrow \mathbb{R}^k$ defined by*

$$u^*(s) = \begin{cases} 0 & \text{if } 0 \leq s < \tau - T \\ u & \text{if } \tau - T \leq s \leq \tau \end{cases} \quad (63)$$

is a step control that steers the solution of (2) from $x^0 \in \mathbb{R}^d$ to $x^1 \in \mathbb{R}^d$ over the time interval $[0, \tau]$.

As is Section III-B1, one has the following important remark.

Remark III.25. Observe that the control synthesis in Proposition III.23 is implicit, as $\kappa(T)$ and $\eta(T)$ incorporate the state $x(s)$ within the integral. However, for a sufficiently small time horizon $T > 0$, if it exists, the feedforward control input $\tilde{u} \in \mathbb{R}^k$, solving

$$B\tilde{u} = \mathcal{C}_T(x^0)(x^1 - \Phi_T(x^0)) =: I \quad (64)$$

provides a first approximation to the control input $u \in \mathbb{R}^k$ that solves (60). Thanks to (49), one has

$$I = D\Psi_T(\Phi_T(x^0)) \left(\text{Id} - e^{-T\mathcal{A}_T(x^0)} \right)^{-1} \mathcal{A}_T(x^0)(x^1 - \Phi_T(x^0)).$$

where $\mathcal{A}_T(x^0) := DN(\Phi_T(x^0))$. It follows that if $I \in \text{Im}(B)$, then (64) has at least one solution, and the constant control $\tilde{u} = B^+I \in \mathbb{R}^k$ is the least-norm solution to (64), and serves as a first approximation to the constant control $u \in \mathbb{R}^k$ synthesized in Proposition III.23. This control \tilde{u} approximately steers the solution of (2) from x^0 to x^1 over the time interval $[0, T]$, provided $T > 0$ is sufficiently small.

Interestingly, the control $\tilde{u} \in \mathbb{R}^k$ is actually a solution of

$$\left(\text{Id} - e^{-T\mathcal{A}_T(x^0)} \right) D\Phi_T(x^0)B\tilde{u} = \mathcal{A}_T(x^0)(x^1 - \Phi_T(x^0)). \quad (65)$$

Hence, similar to the analysis performed in Remark III.5, one can study the eigenvalues of $DN(x^0)$ —by Lemma III.21—to derive more general conditions that guarantee the existence of $\tilde{u} \in \mathbb{R}^k$ satisfying (65) when $\|W\| \geq \lambda_{\min}(D)$.

For more details on the accuracy of this approximation, we refer the reader to Section IV, where numerical simulations are presented.

C. General comments on the main results

It is worth noticing that (2) is more general than [24, Eq. (2)] in many aspects. In the latter, the drift term is $N(x) = Af(x)$ where A is a squared matrix, and the transfer function f is bounded and odd and, more generally, belongs to a set of functions that is more restrictive than that considered here albeit with the smoothness assumption on f . Moreover, the input matrix B is also assumed to belong to some open and dense subset of $\mathcal{M}_{n,k}(\mathbb{R})$, a hypothesis that we do not explicitly assume here. Consequently, the control synthesis that

we provide here applies to [24, Eq. (2)] when the decay matrix $D = 0$. More generally, our control synthesis can be applied to delay-free nonlinear drift terms in Lur’e form.

The spectral norm condition $\|W\| < \lambda_{\min}(D)$ in the main results presented in Theorems III.2, III.6 and III.18 makes (2) a contracting system. Indeed, it is straightforward to show that under this condition, (2) admits a unique equilibrium for every input $u \in \mathbb{R}^k$, which is globally exponentially stable. Contracting inherent dynamics enjoy interesting properties [14] and have been widely assumed (not the $\|W\| < \lambda_{\min}(D)$ condition, but the contracting assumption generally) in many recurrent neural networks studied [4], [8]. Therefore, our control syntheses may be applied in many instances.

Remark III.26 (On the regularity assumptions on f_i). Many of the results presented in this paper hold under the assumption that the activation function f_i is C^1 and globally Lipschitz continuous on \mathbb{R} . For instance, the solution representations in Theorems II.2 and II.4 are still valid, but in this case, the solution x is C^2 in t . In particular, the key results given in Lemmas III.9, III.10, and III.21 remain valid.

Note that if f_i is only globally Lipschitz on \mathbb{R} and C^1 —and not C^2 (in this case, the solution x is C^2 in t , not C^3), then Propositions III.7 and III.19 (then Theorems III.6 and III.18) remain valid whenever the *upper* Dini derivative $D^+ f'_i$ of f'_i is bounded *everywhere*. The latter is crucial since the matrices ζ and φ will contain the Dini Hessian matrix $D^{+2} f := D^+ Df$ (Df being the Jacobian of f) of f as a multiplicative factor under the integral sign. Therefore, the series defining ζ and φ converge in $\mathcal{M}_d(\mathbb{R})$ if and only if the spectral norm of $D^{+2} f$ is bounded *everywhere*.

Furthermore, if f_i is only globally Lipschitz on \mathbb{R} , then, say, (26) cannot be used as the expansion of $x(t)$. The issue here is not only ζ , which is no longer well-defined but also the Dini derivative $D^+ N$ is not continuous, making the r.h.s. of (26) not a C^1 function in t .

IV. EXAMPLES AND NUMERICAL SIMULATIONS

This section presents some numerical simulations that bolster our theoretical study.

A. Implementation

We implemented the synthesis for linear (17) and nonlinear (45) systems in `python` using the `torchdiffeq` package [6]. The scripts will be available after publication. For nonlinear systems, we presented the results for (45) instead of (III.25), because we found that the matrix $\text{Id} - e^{-T A x(x^0)}$ in (III.25) became ill-conditioned for large T and led to large numerical error, while (45) did not suffer from this issue. We only considered the case where $k = d$ and $B = \text{Id}$, since the extension to $u = B^+ I$ is straightforward, for instance, when B is full row rank. For nonlinear systems, we numerically integrated the ODE using the `odeint()` function with default parameters, which utilizes a Runge-Kutta method of order 5 of Dormand-Prince-Shampine. The algorithm accepts a new step if $\text{RMS}(\varepsilon) < 10^{-9} + 10^{-7} * \text{RMS}(x)$, where RMS represents the root mean square norm, ε being the estimated

error and x the current state. The Jacobian of the flow with respect to the initial state was computed through automatic differentiation in `pytorch`. Experiments were conducted on a desktop computer with an Nvidia RTX 3080 GPU. The run time for each synthesis increased as the time horizon T and number of features (neurons) d increased but remained within the scope of several hundred milliseconds to several seconds (see Figure 4, 5). For a fixed T and multiple desired trajectories (i.e., different pairs of (x^0, x^1)), the synthesis is efficiently parallelized, and the run time remains almost constant when increasing the number of trajectories from one to as many as 1000.

To construct a d -dimensional linear system, we randomly sampled the entries of W from the normal distribution $\mathcal{N}(0, 1/d)$. The decay matrix was set to $(\lambda_{\max}(W) - \lambda_0) \text{Id}$, where $\lambda_{\max}(W) \in \mathbb{R}$ is the maximum of the real parts of the eigenvalues of W and $\lambda_0 \in \mathbb{R}$ is the desired maximum real part of the eigenvalues of the dynamic matrix $A = W - D$. We tried both $\lambda_0 = -0.1$ and $\lambda_0 = 0.1$ to construct stable and unstable systems respectively. To construct a nonlinear RNN, we set $D = \text{Id}$ and the activation function to \tanh . We followed [23] and imposed a “random plus low rank” structure on the connectivity matrix $W = J + \mathbf{m}\mathbf{n}^T$. The matrix $J \in \mathbb{R}^{d \times d}$ was sampled from the normal distribution $\mathcal{N}(0, g^2/d)$, where $g = 0.9$ is a scaling factor. $\mathbf{m} \in \mathbb{R}^{d \times 1}$ were sampled from standard normal distribution. $\mathbf{n} \in \mathbb{R}^{d \times 1}$ is either sampled from normal distribution $\mathcal{N}(0, 1/d^2)$ or set as $\mathbf{n} = \frac{1.1}{d} \mathbf{m}$. It can be shown that the system is monostable in the first case and bistable in the second case [23]. Such type of model appears frequently in theoretical neuroscience studies [16].

To further evaluate the method on realistic models fit to *experimental data*, we also included a set of Mesoscale Individualized Neurodynamic (MINDy) models from [20]. MINDy models contained 100 interconnected units representing 100 brain areas, and the parameters were optimized to approximate the activation time series of these areas measured through functional magnetic resonance imaging (fMRI). Unlike most RNNs, the activation function of MINDy is heterogeneous: $f(s) = \sqrt{\alpha^2 + (bs + 0.5)^2} - \sqrt{\alpha^2 + (bs - 0.5)^2}$, where $b = 20/3$ is fixed and α is optimized over the data and differs across the 100 units. It is also worth noting that the origin is unstable in most of the MINDy models, indicating that the spectral norm condition $\|W Df(0)\| < \lambda_{\min}(D)$ was not met. However, we found that the models satisfied the eigenvalue condition, which enabled the synthesis.

We analyzed the endpoint error of the controlled trajectory for $T = 2^{-2}, 2^{-1}, \dots, 2^7$. For each T , we randomly generated 5 stable and 5 unstable linear systems, 5 monostable and 5 bistable \tanh RNNs, and randomly selected 5 fitted MINDy models (from a pool of 106 models). All models were 100-dimensional. Then, we randomly sampled 20 pairs of (x^0, x^1) from standard normal distribution for each system. Input synthesis was computed using either the nonlinear method (equation (45)) or the ‘linearized’ method described below:

For the nonlinear system (2), the “linearized” system at x^0 is given by:

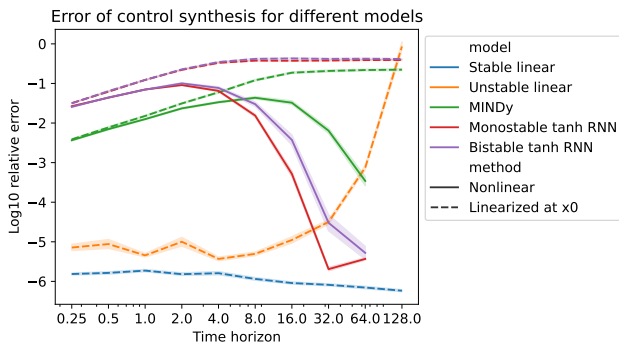


Fig. 2. **Relative endpoint error under synthesized input.** The x -axis (log scale) indicates the time horizon T . The y -axis represents the common logarithm of the ratio between the Euclidean norm of endpoint error $x(T) - x^1$ and the Euclidean norm of $x^1 - x^0$. Line style indicates the method used for synthesis, and color indicates different types of models. The error band represents a 95% confidence interval of the mean log relative error for each combination of time horizon, model, and method. The missing value for the nonlinear method for large T was due to the underflow of the numerical integration, which can be mitigated by increasing the error tolerance.

$$\dot{\hat{x}}(t) = DN(x^0)\hat{x}(t) + N(x^0) + I \quad (66)$$

where $\hat{x}(t)$ is the approximation of $x(t) - x^0$. Using (17), the following input I drives the linearized system from $\hat{x}^0 = \mathbf{0}$ to $\hat{x}^1 = x^1 - x^0$ in exact time T :

$$I = (e^{TA} - \text{Id})^{-1} A (x^1 - x^0) - N(x^0) \quad (67)$$

where $A = DN(x^0)$. We have also tried to linearize the systems at the origin (which is always a fixed point) and obtained qualitatively similar results.

B. Results

Results were summarized in Figure 2. The full distribution of the error across all trials was visualized in Figure 3. For stable linear systems, the error remained small. For unstable linear systems, as T increased, the numerical error for computing the inverse of $e^{TA} - \text{Id}$ became very large as it will have both very large eigenvalues and eigenvalues close to -1 . For nonlinear systems, the linearized method is effective only for small T (as expected). In contrast, and encouragingly, the nonlinear method performed well for all T , regardless of whether the system had monostable or more complicated dynamics. Interestingly, with the nonlinear method, the error even decreased as T increased. It is worth noting that the synthesis for the MINDy model was very accurate even at $T = 80$ (see Figures 6), corresponding to almost one minute of physical time.

V. CONCLUSION

In this paper, we investigated the control synthesis problem for a class of nonlinear Hopfield-type recurrent neural networks motivated by applications in neurostimulation. By using a solution representation that generalizes Duhamel's principle, we derived constant and piecewise constant inputs that drive the network to a desired target state within specified

time intervals. In the case of linear activation functions, we demonstrated that the network is controllable over arbitrary time horizons if certain conditions on the decay and connectivity matrices are satisfied. Numerical examples validated the theoretical results and highlighted the practical potential of the proposed approach in guiding the design of transcranial electrical stimulation protocols.

Future work will extend these methods to synthesizing time-varying control input and investigate their robustness under parameter uncertainty and external disturbances. Indeed, large-scale models, such as (2), are highly sensitive to external noise and disturbances. Thus, it is crucial to design a time-varying control input that not only achieves the control objective but also dynamically adapts to external perturbations while minimizing the energy cost. This challenge extends beyond the control synthesis problem to include considerations of energetic performance. This latter question is ongoing in [25].

APPENDIX

This section contains various complements used in the previous sections. The first result concerns some useful properties of the nonlinear vector field N .

Lemma A.1. *The nonlinear vector field N defined in (3) belongs to $C^2(\mathbb{R}^d; \mathbb{R}^d)$, and it is Lipschitz continuous from \mathbb{R}^d into itself. Moreover, the following holds*

$$\begin{aligned} DN(x) &= -D + WDf(x) \\ \|DN(x)\| &\leq \lambda_{\max}(D) + \|W\| \end{aligned} \quad \forall x \in \mathbb{R}^d. \quad (68)$$

$$\begin{aligned} D^2N(x) &= WD^2f(x) \\ \|D^2N(x)\| &\leq \|f''\|_{\infty} \|W\| \end{aligned} \quad \forall x \in \mathbb{R}^d. \quad (69)$$

Here $\|f''\|_{\infty} := \max_{i \in [1, d]} \|f''_i\|_{\infty}$, $Df(x) = (f'_i(x_i)\delta_{i,j})$ and $D^2f(x)$ is a third order tensor such that $D^2f(x)yz \in \mathbb{R}^d$ for all $y, z \in \mathbb{R}^d$, and the i -th element is given, by

$$[D^2f(x)yz]_i = \sum_{j,k=1}^d \frac{\partial^2 f_i}{\partial x_j \partial x_k}(x) y_j z_k = f''_i(x_i) y_i z_i. \quad (70)$$

Proof. Let $x, y \in \mathbb{R}^d$. Since $\|Df(x)\| \leq 1$, one has

$$\|f(x) - f(y)\|_2 \leq \|Df(x)\| \|x - y\|_2 \leq \|x - y\|_2. \quad (71)$$

One deduces that

$$\|N(x) - N(y)\|_2 \leq (\lambda_{\max}(D) + \|W\|) \|x - y\|_2 \quad (72)$$

showing that N is globally Lipschitz continuous from \mathbb{R}^d into itself. On one hand, one has obviously that $N \in C^2(\mathbb{R}^d; \mathbb{R}^d)$ since $f \in C^2(\mathbb{R}^d; \mathbb{R}^d)$ by assumption. It follows that $DN(x)h = -Dh + WDf(x)h$ is linear w.r.t. $h \in \mathbb{R}^d$ and satisfies

$$\|DN(x)h\|_2 \leq (\lambda_{\max}(D) + \|W\|) \|h\|_2$$

so that (68) is satisfied. On the other hand, for all $y, z \in \mathbb{R}^d$, one has

$$D^2N(x)yz = WD^2f(x)yz.$$

Since $f : \mathbb{R}^d \rightarrow \mathbb{R}^d$, $D^2f(x)$ is a third order tensor, one has $D^2f(x)yz \in \mathbb{R}^d$ for all $y, z \in \mathbb{R}^d$. Therefore, (70) is satisfied

because of the ‘‘diagonal’’ structure of f , the second partial derivatives of f_i are non-zero only when $j = k = i$. It follows by Cauchy-Schwarz inequality that

$$\|D^2 f(x)yz\|_2 \leq \|f''\|_\infty \|W\| \|y\|_2 \|z\|_2$$

where $\|f''\|_\infty := \max_{i \in [1, d]} \|f''_i\|_\infty$. \square

The next result concerns the differential of the flow Φ of the vector field N .

Lemma A.2. *Assume that f_i is a C^1 global Lypchitz function on \mathbb{R} . For every $t \in \mathbb{R}$, the differential $D\Phi_t(x)$ of the flow Φ_t is a well-defined invertible matrix, and it holds*

$$\begin{aligned} \|D\Phi_t(x)\| &\leq e^{\Lambda|t|} \\ \|D\Psi_t(y)\| &\leq e^{\Lambda|t|} \end{aligned} \quad (73)$$

for all $x \in \mathbb{R}^d$, $y = \Phi_t(x)$ and $\Lambda := \lambda_{\max}(D) + \|W\|$.

Proof. The vector field N is a C^1 globally Lipschitz function on \mathbb{R}^d . Then, its flow Φ_t is well-defined and invertible for any $t \in \mathbb{R}$. Denoting Ψ_t its inverse, one has that Φ_t and Ψ_t are C^1 and globally Lypchitz function on \mathbb{R}^d , and it holds

$$[D\Phi_t(x)]^{-1} = D\Psi_t(y) \quad \text{for } y = \Phi_t(x). \quad (74)$$

Fix $z \in \mathbb{R}^d$ and introduce for $s \in \mathbb{R}$, $b(s) = D\Phi_s(x)z$. Then, $b \in C^1([0, \infty); \mathbb{R}^d)$ and it holds

$$\begin{aligned} \frac{1}{2} \frac{d}{ds} \|b(s)\|_2^2 &= \langle \partial_s D\Phi_s(x)z, D\Phi_s(x)z \rangle \\ &= \langle DN(\Phi_s(x))D\Phi_s(x)z, D\Phi_s(x)z \rangle. \end{aligned} \quad (75)$$

It follows by the Cauchy-Schwarz inequality that

$$\left| \frac{1}{2} \frac{d}{ds} \|b(s)\|_2^2 \right| \leq \Lambda \|b(s)\|_2^2 \quad \forall s \in \mathbb{R}. \quad (76)$$

Integrating inequalities (76) on $[0, t]$ for $t \geq 0$, and on $[t, 0]$ for $t \leq 0$ yields to

$$e^{-2\Lambda|t|} \|z\|_2^2 \leq \|D\Phi_t(x)z\|_2^2 \leq e^{2\Lambda|t|} \|z\|_2^2. \quad (77)$$

for every $t \in \mathbb{R}$. This completes the proof of the lemma. \square

It should be noted that $\|D\Phi_t(x)\|$ does not systematically grow with $t \geq 0$ as one might think by examining (73). Indeed, one can prove—by replacing $DN(\Phi_s(x))$ by its expression in (75), and proceed as in (81) below—the following.

Lemma A.3. *For every $t \geq 0$, it holds*

$$\begin{aligned} \|D\Phi_t(x)\| &\leq e^{-(\lambda_{\min}(D) - \|W\|)t} \\ \|D\Psi_t(y)\| &\geq e^{-(\lambda_{\min}(D) - \|W\|)t} \end{aligned} \quad (78)$$

where $x \in \mathbb{R}^d$ and $y = \Phi_t(x)$.

One also has the following result.

Lemma A.4. *Set $A = -D + W$. If $\|W\| \leq \lambda_{\min}(D)$, then it holds*

$$\|e^{tA}\| \leq 1 \quad \forall t \geq 0. \quad (79)$$

In particular, if $\|W\| < \lambda_{\min}(D)$, then

$$\|e^{tA}\| < 1 \quad \forall t > 0. \quad (80)$$

Proof. Let $x \in \mathbb{R}^d \setminus \{0\}$. Then, one has

$$\begin{aligned} \langle Ax, x \rangle &= -\langle Dx, x \rangle + \langle Wx, x \rangle \\ &\leq -(\lambda_{\min}(D) - \|W\|) \|x\|_2^2 \leq 0. \end{aligned} \quad (81)$$

It follows that the matrix A is dissipative and that for every $x \in \mathbb{R}^d$, the map $t \in [0, \infty) \mapsto \|e^{tA}x\|_2^2$ is non-increasing, completing the proof of (79). Furthermore, if $\|W\| < \lambda_{\min}(D)$, then one deduces from (81) that the map $t \mapsto \|e^{tA}x\|_2^2$ is strictly decreasing, and (80) follows. \square

In the following lemma, one shows that the three series in Proposition III.7 are well-defined.

Lemma A.5. *The series (26), (27) and (28) in Proposition III.7 are well-defined in $\mathcal{M}_d(\mathbb{R})$. Moreover, the spectral norms of $\xi(t)$ and $\chi(t)$ satisfy*

$$\|\xi(t)\| \leq C \|I\|_2 t^3 e^{3\Lambda t} \quad (82)$$

$$\|\chi(t)\| \leq C [\Lambda e^{\Lambda t} \|x^0\|_2 + (\Lambda t e^{\Lambda t} + 1) \|I\|_2] t^3 e^{3\Lambda t} \quad (83)$$

for all $u \in \mathbb{R}^k$ and $t \geq 0$. Here $I = Bu$, $\Lambda := \lambda_{\max}(D) + \|W\|$, $\|f''\|_\infty := \max_{i \in [1, d]} \|f''_i\|_\infty$ and $C := \|W\| \|f''\|_\infty$.

Proof. For every $n \in \mathbb{N}$, one has $1/(n+1) \leq 1$ so that

$$\left\| \sum_{n=0}^{\infty} \frac{t^{n+1} Z_t^n}{(n+1)!} \right\| \leq t \sum_{n=0}^{\infty} \frac{t^n \Lambda^n}{n!} = t e^{\Lambda t} \quad \forall t \geq 0 \quad (84)$$

since $Z_t := DN(\Psi_t(x(t)))$ satisfies $\|Z_t^n\| \leq \Lambda^n$ by Lemma A.1. It follows that the series in (26) defined an element of $\mathcal{M}_d(\mathbb{R})$. One also has

$$\frac{d}{ds} Z_s^n = \sum_{k=1}^n Z_s^{k-1} \dot{Z}_s Z_s^{n-k} \quad (85)$$

so that for every $n \geq 1$, it holds

$$\left\| \frac{d}{ds} Z_s^n \right\| \leq n \|Z_s\|^{n-1} \|\dot{Z}_s\| \leq n \Lambda^{n-1} \|\dot{Z}_s\|. \quad (86)$$

Furthermore, $\dot{Z}_s = WD^2 f(\Psi_s(x(s)))P_s I$, and it holds

$$\begin{aligned} \|\xi(t)y\|_2 &\leq C \|I\|_2 \|y\|_2 \sum_{n=1}^{\infty} \int_0^t \frac{s^{n+1}}{(n+1)!} n \Lambda^{n-1} e^{2\Lambda s} ds \\ &\leq C \|I\|_2 t^3 e^{3\Lambda t} \|y\|_2 \end{aligned}$$

for all $y \in \mathbb{R}^d$ by Lemmas A.1 and A.2. Here $C := \|W\| \|f''\|_\infty$. Let us prove (83). Firstly, one has $\dot{x}(s) = N(x(s)) + I$ so that $\|\dot{x}(s)\|_2 \leq \Lambda \|x(s)\|_2 + \|I\|_2$ since $N(0) = 0$ and N is Λ -Lipschitz by Lemma A.1. Therefore, by Cauchy-Schwarz inequality

$$\begin{aligned} \frac{d}{ds} \|x(s)\|_2 &= \frac{\langle \dot{x}(s), x(s) \rangle}{\|x(s)\|_2} \leq \|\dot{x}(s)\|_2 \\ &\leq \Lambda \|x(s)\|_2 + \|I\|_2 \end{aligned} \quad (87)$$

which, by Gronwall's lemma, implies that

$$\begin{aligned} \|x(s)\|_2 &\leq e^{\Lambda s} \|x^0\|_2 + \|I\|_2 \int_0^s e^{\Lambda s} e^{-\Lambda \tau} d\tau \\ &\leq e^{\Lambda s} \|x^0\|_2 + s e^{\Lambda s} \|I\|_2. \end{aligned} \quad (88)$$

It follows that

$$\|\dot{x}(s)\|_2 \leq \Lambda e^{\Lambda s} \|x^0\|_2 + \Lambda s e^{\Lambda s} \|I\|_2 + \|I\|_2. \quad (89)$$

Secondly, the hessian matrix $D^2\Psi_s(x(s))$ solves the integral equation

$$\begin{aligned} D^2\Psi_s(x(s)) &= - \int_0^s DN(\Psi_\tau(x(s))) D^2\Psi_\tau(x(s)) d\tau \\ &\quad - \int_0^s D^2N(\Psi_\tau(x(s))) D\Psi_\tau(x(s)) D\Psi_\tau(x(s)) d\tau. \end{aligned} \quad (90)$$

Using (73) and (69), one gets

$$\begin{aligned} \|\|D^2\Psi_s(x(s))\|\| &\leq \Lambda \int_0^s \|\|D^2\Psi_\tau(x(s))\|\| d\tau \\ &\quad + C \int_0^s e^{2\Lambda\tau} d\tau \end{aligned} \quad (91)$$

which, by Gronwall's lemma, yields to

$$\|\|D^2\Psi_s(x(s))\|\| \leq C \int_0^s e^{2\Lambda\tau} e^{\Lambda s} e^{-\Lambda\tau} d\tau \leq C s e^{2\Lambda s} \quad (92)$$

where $C := \|\|W\|\| \|f''\|_\infty$. Since $\|\|Z_s\|\| \leq \Lambda$, one gets from (28), (89) and (92) that

$$\begin{aligned} \|\chi(t)y\|_2 &\leq C \|x^0\|_2 \|y\|_2 \sum_{n=1}^{\infty} \int_0^t \frac{s^{n+1} \Lambda^n}{n!} e^{3\Lambda s} ds \\ &\quad + C \|I\|_2 \|y\|_2 \sum_{n=1}^{\infty} \int_0^t \frac{s^{n+2} \Lambda^n}{n!} e^{3\Lambda s} ds \\ &\quad + C \|I\|_2 \|y\|_2 \sum_{n=1}^{\infty} \int_0^t \frac{s^{n+1} \Lambda^{n-1}}{n!} e^{2\Lambda s} ds \\ &\leq C [\Lambda e^{\Lambda t} \|x^0\|_2 + (\Lambda t e^{\Lambda t} + 1) \|I\|_2] t^3 e^{3\Lambda t} \|y\|_2. \end{aligned}$$

for all $y \in \mathbb{R}^d$. This completes the proof of (83) and then of the lemma. \square

The following results were also useful in the main text of this paper.

Lemma A.6. *Let $x \in \mathbb{R}^d$. Consider the matrix $\mathcal{B}(x) := DN(x)$. Then, it holds*

$$\|\|e^{t\mathcal{B}(x)}\|\| \leq e^{-(\lambda_{\min}(D) - \|\|W\|\|)t} \quad \forall t \geq 0. \quad (93)$$

In particular, if $\|\|W\|\| < \lambda_{\min}(D)$, it holds

$$\|\|e^{t\mathcal{B}(u)}\|\| \leq e^{-(\lambda_{\min}(D) - \|\|W\|\|)t} < 1 \quad \forall t > 0. \quad (94)$$

Proof. Let $v \in \mathbb{R}^d$, and introduce for every $t \geq 0$, the map $g(t) = e^{t\mathcal{B}(x)}y$. Then, $g \in C^1([0, \infty); \mathbb{R}^d)$, $g(0) = y$ and

$$\dot{g}(t) = \mathcal{B}(x)g(t) = -Dg(t) + W Df(x)g(t) \quad (95)$$

from which one deduces the following integral representation

$$g(t) = e^{-tD}y + \int_0^t e^{-(t-s)D} W Df(x)g(s) ds. \quad (96)$$

Recall that $\|\|Df(x)\|\| \leq 1$. By taking the Euclidean norm of (96), one gets

$$e^{t\lambda_{\min}(D)} \|g(t)\|_2 \leq \|y\|_2 + \|\|W\|\| \int_0^t e^{s\lambda_{\min}(D)} \|g(s)\|_2 ds$$

which by Gronwall's lemma yields to the following.

$$\|g(t)\|_2 \leq e^{-t(\lambda_{\min}(D) - \|\|W\|\|)} \|y\|_2. \quad (97)$$

This completes the proof of the lemma. \square

REFERENCES

- [1] F. Albertini and E. D. Sontag, "For neural networks, function determines form," *Neural Networks*, vol. 6, no. 7, pp. 975–990, 1993.
- [2] T. O. Bergmann, S. Groppa, M. Seeger, M. Mölle, L. Marshall, and H. R. Siebner, "Acute changes in motor cortical excitability during slow oscillatory and constant anodal transcranial direct current stimulation," *Journal of Neurophysiology*, vol. 102, no. 4, pp. 2303–2311, 2009.
- [3] M. Breakspear, "Dynamic models of large-scale brain activity," *Nature Neuroscience*, vol. 20, no. 3, pp. 340–352, 2017.
- [4] V. Centorrino, A. Gokhale, A. Davydov, G. Russo, and F. Bullo, "Euclidean contractivity of neural networks with symmetric weights," *IEEE Control Systems Letters*, vol. 7, pp. 1724–1729, 2023.
- [5] R. Chen, M. Singh, T. S. Braver, and S. Ching, "Dynamical models reveal anatomically reliable attractor landscapes embedded in resting-state brain networks," bioRxiv, 2024.
- [6] R. T. Q. Chen, Y. Rubanova, J. Bettencourt, and D. Duvenaud, "Neural Ordinary Differential Equations," *Advances in Neural Information Processing Systems*. 2018.
- [7] J. M. Coron, *Control and nonlinearity*. No. 136, American Mathematical Soc, 2007.
- [8] A. Davydov, A. V. Proskurnikov and F. Bullo (2022, June). "Non-Euclidean contractivity of recurrent neural networks." In *2022 American Control Conference (ACC)* (pp. 1527-1534). IEEE.
- [9] C. M. DeGiorgio, and S. E. Krahl, "Neurostimulation for drug-resistant epilepsy," *Continuum: Lifelong Learning in Neurology*, vol. 19, no. 3, pp. 743–755, 2013.
- [10] M. Forti and A. Tesi, "New conditions for global stability of neural networks with application to linear and quadratic programming problems," *IEEE Transactions on Circuits and Systems I: Fundamental theory and applications*, vol. 47, no. 7, pp. 354–366, 1995.
- [11] S. Grover, W. Wen, V. Viswanathan, C. T. Gill, and R. MG, Reinhart, "Long-lasting, dissociable improvements in working memory and long-term memory in older adults with repetitive neuromodulation," *Nature Neuroscience*, vol. 25, no. 9, pp. 1237–1246, 2022.
- [12] S. Gu, F. Pasqualetti, M. Cieslak, Q. K. Telesford, A. B. Yu, A. E. Kahn, J. D. Medaglia, J. M. Vettel, M. B. Miller, and S. T. Grafton, and others, "Controllability of structural brain networks," *Nature Communications*, vol. 6, no. 1, pp. 8414, 2015.
- [13] J. J. Hopfield, "Neurons with graded response have collective computational properties like those of two-state neurons," *Proceedings of the National Academy of Sciences*, vol. 81, no. 10, pp. 3088–3092, 1984.
- [14] W. Lohmiller and J. J. E. Slotine. "On contraction analysis for nonlinear systems," *Automatica*, vol. 34, no. 6, pp. 683–696, 1998.
- [15] V. López-Alonso, B. Cheeran, D. Río-Rodríguez, and M. Fernández-del-Olmo, "Inter-individual variability in response to non-invasive brain stimulation paradigms," *Neuron*, vol. 7, no. 3, pp. 372–380, 2014.
- [16] F. Mastroiuseppe, and S. Ostojic, "Linking connectivity, dynamics, and computations in low-rank recurrent neural networks," *Neuron*, vol. 99, no. 3, pp. 609–623, 2018.
- [17] S. F. Muldoon, F. Pasqualetti, S. Gu, M. Cieslak, S. T. Grafton, J. M. Vettel, and D. S. Bassett, "Stimulation-based control of dynamic brain networks," *PLoS Computational Biology*, vol. 12, no. 9, pp. e1005076, 2016.
- [18] J. D. Power, B. L. Schlaggar, C. N. Lessov-Schlaggar, and S. E. Petersen, "Evidence for hubs in human functional brain networks," *Neuron*, vol. 79, no. 4, pp. 798–813, 2013.
- [19] M. F. Singh, A. Wang, M. Cole, S. Ching, T. S. Braver, "Enhancing task fMRI preprocessing via individualized model-based filtering of intrinsic activity dynamics," *NeuroImage*, vol. 247, pp. 118836, 2022.
- [20] M. F. Singh, T. S. Braver, M. W. Cole, and S. Ching, "Estimation and validation of individualized dynamic brain models with resting-state fMRI," *NeuroImage*, vol. 221, pp. 117046, 2020.
- [21] M. F. Singh, Matthew, A. Wang, Anxu, T. S. Braver, and S. Ching, "Scalable surrogate deconvolution for identification of partially-observable systems and brain modeling," *Journal of neural engineering*, vol. 17, no. 4, pp. 046025, 2020.

- [22] S. J. Schiff, *Neural control engineering: the emerging intersection between control theory and neuroscience*, MIT Press, 2011.
- [23] F. Schuessler, A. Dubreuil, F. Mastrogiuseppe, S. Ostojic, and O. Barak, “Dynamics of random recurrent networks with correlated low-rank structure”, *Physical Review Research*, vol. 2, no. 1, pp. 013111, 2020.
- [24] E. D. Sontag, and Y. Qiao, “Remarks on controllability of recurrent neural networks”, *Proceedings of the IEEE Conference on Decision and Control*, Vol. 1. Institute of Electrical and Electronics Engineers Inc., 1998.
- [25] C. Tamekue, R. Chen, and S. Ching, “Controllability of large scale brain dynamics: Reachability, robustness, and energy efficiency”, *In preparation*.
- [26] C. Tamekue, D. Prandi, and Y. Chitour, “A mathematical model of the visual MacKay effect”, *SIAM Journal on Applied Dynamical Systems*, vol. 23, no. 3, pp. 2138–2178, 2024.
- [27] Z. Yi, P.-A. Heng, and A. W.-C. Fu, “Estimate of exponential convergence rate and exponential stability for neural networks”, *IEEE Transactions on Neural Networks*, vol. 10, no. 6, pp. 1487–1493, 1999.
- [28] H. Zhang, Z. Wang, and D. Liu, “A comprehensive review of stability analysis of continuous-time recurrent neural networks”, *IEEE Transactions on Neural Networks and Learning Systems*, vol. 25, no. 7, pp. 1229–1262, 2014. doi: 10.1109/TNNLS.2014.2317880.

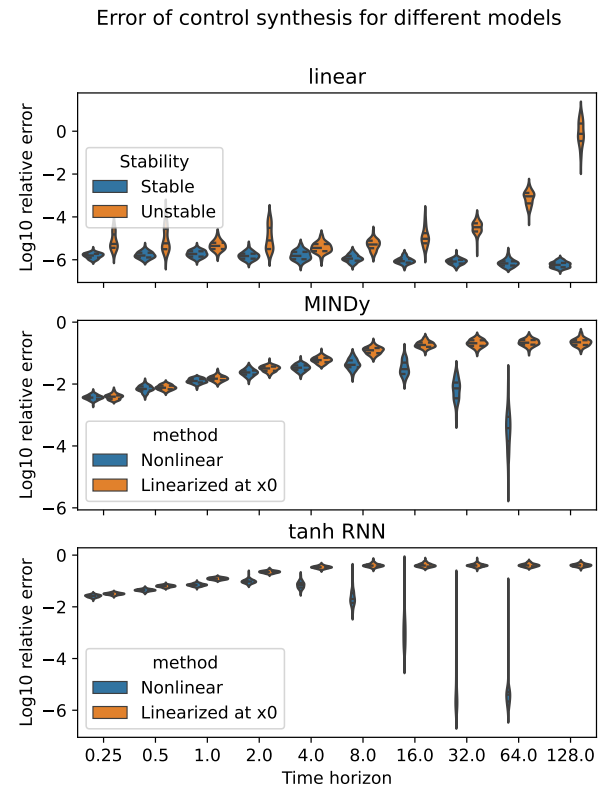


Fig. 3. **Distribution of relative endpoint error across all trials.** We combined the monostable and bistable tanh RNNs as they showed similar patterns.

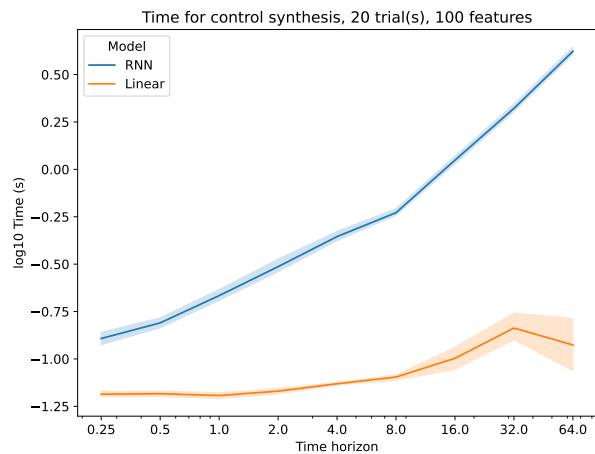


Fig. 4. **Run time for the numerical synthesis for different time horizons.** Results were plotted for random linear systems (using the linear method) and random tanh RNNs (using the nonlinear method), respectively. Experimental details and figure annotations were the same as main figure 2.

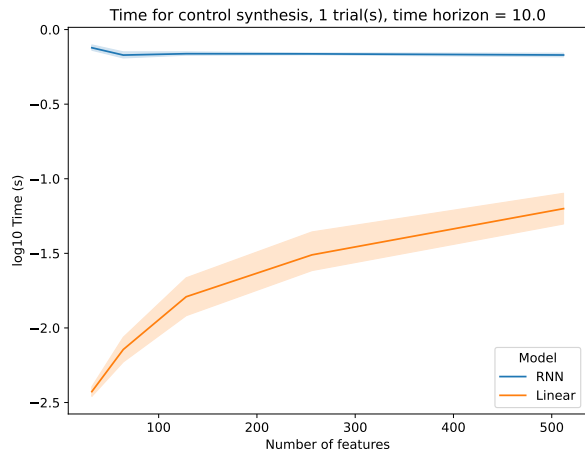


Fig. 5. Run time for the numerical synthesis for different numbers of neurons/features.

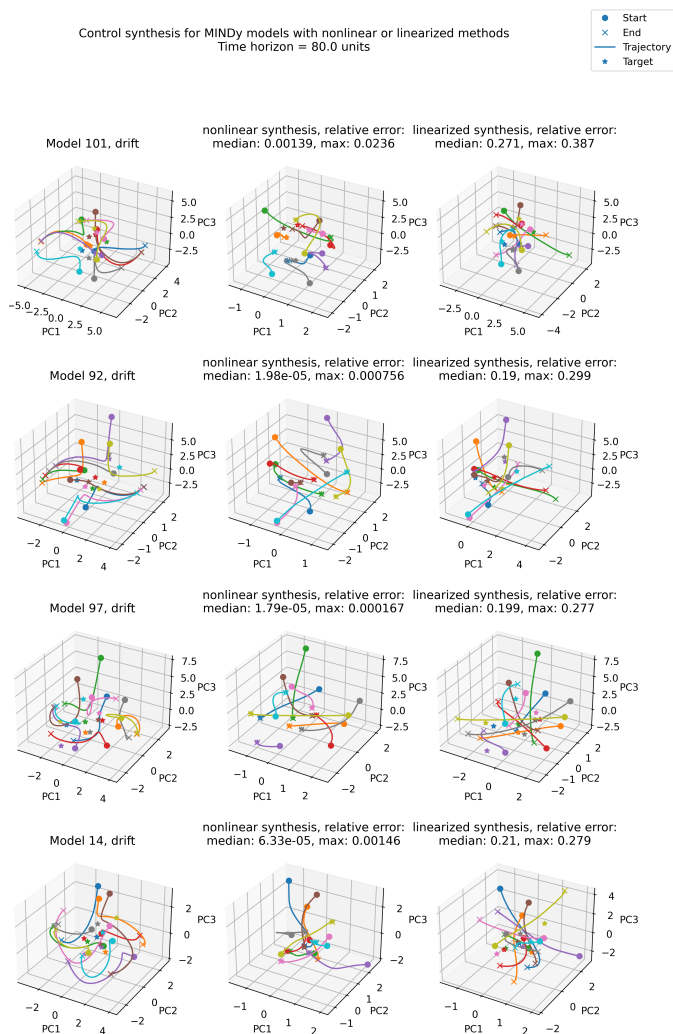


Fig. 6. Examples of synthesized controlled trajectories in MINDy models. Each row represents simulated trajectories starting from x^0 for time T in one model under no input (left), input synthesized using nonlinear flow (middle), and input synthesized using linearized method (right). Trajectories were projected to the first three principal components of the trajectories under no input (left panel in each row).